



Posterior vitreous cortex hyalocytes visualization in asymmetric pigmented paravenous chorioretinal atrophy (PPCRA) using *en face* OCT

Julia Fallon^{a,b}, Sofia Ahsanuddin^{a,b}, Oscar Otero-Marquez^{a,b}, Hernan Andres Rios^{a,b}, Michael M. Park^{a,b}, Toco Y.P. Chui^{a,b}, Richard B. Rosen^{a,b,*}

^a Department of Ophthalmology, New York Eye and Ear Infirmary of Mount Sinai, 310 East 14th Street, New York, NY, 10003, USA

^b Department of Ophthalmology, Icahn School of Medicine at Mount Sinai, One Gustave L. Levy Place, Box 1183, New York, NY, 10029, USA

ARTICLE INFO

Keywords:

Optical coherence tomography (OCT)
OCT Angiography (OCT-A)
Vitreous cortex hyalocytes
Pigmented paravenous chorioretinal atrophy (PPCRA)

ABSTRACT

Purpose: Pigmented paravenous chorioretinal atrophy (PPCRA) is a rare retinal disease with inflammatory or infectious associations affecting the retinal pigment epithelium (RPE) and choriocapillaris. While the clinical manifestations and imaging findings are well-documented in the literature, no reports exist describing potential biomarkers of intraocular inflammation or ischemia in this condition, such as the presence of posterior vitreous cortex hyalocytes.

Observations: We report a case of a 26-year-old female who presented with progressive peripheral vision loss in both eyes over one year. Dilated fundus examination revealed bilateral, asymmetric bone-spicule pigmentary changes along the retinal veins, which appeared more advanced in the left eye. Optical coherence tomography (OCT) revealed the presence of numerous hyalocytes in both eyes 3 μm anterior to the inner limiting membrane (ILM). The morphology of the hyalocytes differed between the two eyes, suggesting different levels of activation related to the stage of the disease. Specifically, the left eye, with more advanced disease, exhibited hyalocytes with multiple elongated processes consistent with a quiescent state, whereas the right eye, with the less advanced disease state, exhibited amoeboid-appearing hyalocytes suggestive of more active inflammation.

Conclusions: This case illustrates how hyalocyte morphology may reflect the underlying activity of an indolent retinal degeneration and provide a useful biomarker of disease progression.

1. Introduction

Pigmented paravenous chorioretinal atrophy (PPCRA) is a rare retinal disease marked by chorioretinal atrophy and pigment clumps following the distribution of the retinal veins.^{1,2} The disease process typically varies from nonprogressive to slowly progressive, and is usually bilateral; however, asymmetry in appearance is common.³ It is often discovered as an incidental finding on examination and its natural course is poorly understood.^{4,5} PPCRA was first described in a case report in 1937 as retinohoroiditis radiata in a 47-year-old man with notable peripapillary atrophy that extended in a radial distribution along the course of the retinal veins.⁶ The disease is more prevalent in males, and the etiology of the condition is unknown; however, it has been hypothesized to have genetic, inflammatory, and infectious associations including sarcoidosis, Behçet's disease, syphilis, tuberculosis, rubella, and measles.^{3,4,6-9} Patients often are asymptomatic or have mildly blurred vision, except for patients who exhibit macular

involvement, for whom central vision may be compromised.¹⁰

Due to the condition's heterogenous phenotype, multimodal imaging is crucial for confirming the diagnosis and monitoring the progression of disease.^{4,8,9,11} Published reports involving fundus autofluorescence (FAF) and spectral domain optical coherence tomography (SD-OCT) have documented the presence of well-demarcated areas of hypoautofluorescence surrounded by a ring of hyperautofluorescence, thinning of the entire outer retina, and reduced choroidal thickness.¹² Optical coherence tomography angiography (OCT-A) has been recently utilized to investigate pathological alterations in vessel density and choriocapillaris porosity in patients with PPCRA.¹²⁻¹⁶ These reports provide evidence of choriocapillaris hypoperfusion and reduced vessel density in the deep capillary plexus of the retina in this condition.^{13,16}

To date, the use of noninvasive imaging to evaluate the natural course and pathogenesis of PPCRA has been limited. Despite the condition's presumed inflammatory or infectious associations, *in vivo* imaging of intraocular biomarkers of inflammation has not been described

* Corresponding author. 310 E. 14th St, New York, NY, 10003, USA.

E-mail address: RRosen@nyee.edu (R.B. Rosen).

<https://doi.org/10.1016/j.ajoc.2023.101846>

Received 1 December 2022; Received in revised form 26 March 2023; Accepted 9 April 2023

Available online 12 April 2023

2451-9936/© 2023 Published by Elsevier Inc. This is an open access article under the CC BY-NC-ND license (<http://creativecommons.org/licenses/by-nc-nd/4.0/>).

thus far in the literature. One potential biomarker involves monitoring the morphology and activity of posterior vitreous cortex hyalocytes, which are macrophage-like cells resident to the dense collagen fibril network of the vitreous base and posterior vitreous cortex anterior to the internal limiting membrane (ILM).^{17,18} Animal studies have demonstrated that hyalocytes perform a myriad of complex functions including immune modulation, antigen processing and presentation, and synthesis of extracellular matrix components that are essential for maintaining vitreous transparency and avascularity.^{19–22} These cells play an integral role in mediating response to inflammation, maintaining homeostasis, and providing neuroprotection.^{23,24} Recent studies have also suggested that hyalocytes serve as mediators of intraocular immunologic homeostasis.^{25,26}

The present case report details the use of clinical *en face* OCT to image hyalocytes *in vivo* in the posterior vitreous cortex of a patient with PPCRA. Furthermore, our case illustrates that this noninvasive imaging modality can identify differences in hyalocyte morphology, which reflect the level of inflammatory activation and may potentially be predictive of disease progression. These examinations were HIPAA compliant and adhered to the tenets of the Declaration of Helsinki. Written informed consent to feature these images were obtained from the patient.

2. Case report

A 26-year-old female with no remarkable past medical history presented to the New York Eye and Ear Infirmary of Mount Sinai with one year of progressive peripheral vision loss worse in the left eye. She reported no known family history of inherited ocular disease and denied nyctalopia. On exam, visual acuity measured 20/20 in each eye. Anterior segment exam was unremarkable and her pupils were briskly reactive without an afferent pupillary defect. Dilated fundus examination was notable for bilateral bone-spicule pigmentation with areas of hypopigmentation and RPE atrophy along the distribution of the retinal veins, worse in the left eye (Fig. 1A and B). Fundus autofluorescence revealed hypoautofluorescence in the areas of atrophy with a surrounding ring of hyperautofluorescence (Fig. 2A and B). SD-OCT was notable for preservation of central foveal contour with loss of outer retinal layers, more significant in the left eye (Fig. 3A and B). Fluorescein angiography revealed staining in the areas of chorioretinal atrophy of both eyes.

En face OCT reflectance (OCT-R) scans with corresponding OCT-A were obtained using a commercial SD-OCT system with a scan rate of 70,000 A-scans per second, scan beam wavelength centered at 840 nm, and a bandwidth of 45 nm (Avanti RTVue-XR; Optovue, Fremont, CA, USA). Two sets of 10 sequential 3 mm × 3 mm OCT scans centered at the fovea and 9° temporal to the fovea of each eye were obtained for a total of 20 scans per study eye (Fig. 4). The foveal images are not included in this manuscript due to the scarcity of hyalocytes visualized on OCT. Following image acquisition, OCT-R and corresponding OCT-A images

were generated using the Optovue AngioAnalytics software (version 2017.1.0) and the XR-Avanti Exporting Tool (version 2019.1.28, Optovue). Image registration and averaging were performed using ImageJ (ImageJ, U.S. National Institute of Health, Bethesda, Maryland, USA). The images were averaged to minimize motion artifacts and improve the signal-to-noise ratio.^{27,28} To correct for ocular magnification of each averaged image, axial length was measured using an IOLMaster (Carl Zeiss Meditec, Dublin, CA, USA). An analysis of the 3 μm slab anterior to the ILM showed numerous hyalocytes located over the retinal surface. In the right eye, the hyalocytes displayed more amoeboid, spherical configurations with fewer retracted processes at both the fovea and the temporal retina. In the left eye, the hyalocytes were characterized by a dispersed nonuniform spatial distribution and a more ramified morphology with elongated, spindle-like processes at both locations. The hyalocytes appear to be more densely concentrated in areas that are currently undergoing chorioretinal degeneration or have already atrophied. To generate the color overlays in Fig. 4, the full retinal vascular layer (ILM to outer plexiform layer (OPL) + 9 μm) and coronal plane *en face* OCT-R slab from ILM to 3 μm immediately anterior to the ILM were used.

Genetic testing through Invitae Inherited Retinal Disorders Panel (Spark Therapeutics Inc., Philadelphia, PA) for the patient was positive for various mutations of undetermined significance in the following genes: HMCN1, LRP5, RBP3, TEAD1 and WDR19. A limited inflammatory and infectious workup was undertaken. Complete blood count, comprehensive metabolic panel, angiotensin-converting enzyme, rheumatoid factor, Quantiferon-TB Gold (QIAGEN, Hilden, Germany), rapid plasma reagin, and fluorescent treponemal antibody absorption testing were all within normal limits. An anti-nuclear antibody titer was positive at 1:80 with speckled pattern. The use of oral steroids was considered in her treatment plan; however, after discussion with the patient, the decision was made to continue observation.

3. Discussion

In this case report, we demonstrate the utility of *en face* OCT to visualize hyalocytes in a patient with bilateral, asymmetric PPCRA. PPCRA is uncommon and multimodal imaging reports have thus been mostly limited to dilated fundus photography, FAF, swept source OCT (SS-OCT), and SD-OCT, and more recently OCT-A imaging findings.^{29,30} In 2021, Jung et al. published a case report detailing wide fluorescein angiography (FA), wide indocyanine green angiography (ICGA), optical coherence tomography angiography (OCT-A), and electroretinogram (ERG) findings in order to help clinicians distinguish PPCRA from other pigmentary retinopathies, such as retinitis pigmentosa, hydroxychloroquine retinopathy, or serpiginous choroidopathy.¹⁵ More recent studies using OCT-A in patients with PPCRA have demonstrated alterations in vessel perfusion and density. Lee et al. describe the OCT-A imaging characteristics of eyes affected by PPCRA.¹² In their studies, they noted relative preservation of retinal perfusion with significant

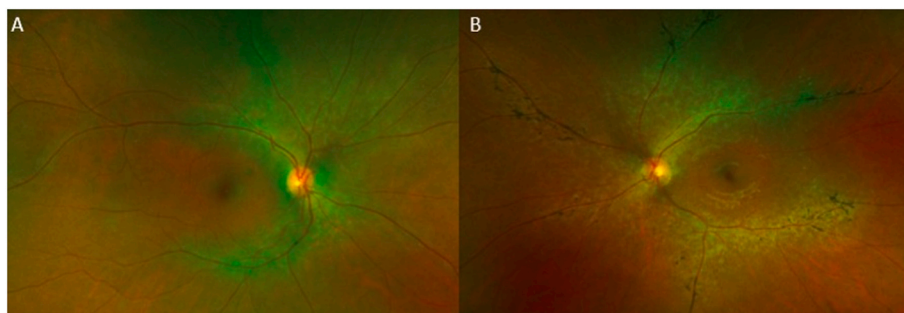


Fig. 1. Fundus images of OD (A) and OS (B) demonstrating asymmetric chorioretinal atrophy surrounding the venous arcades without foveal involvement. The vessels are attenuated OU. Pigment clumps and bone spicules are found distributed along the venous arcades OS.

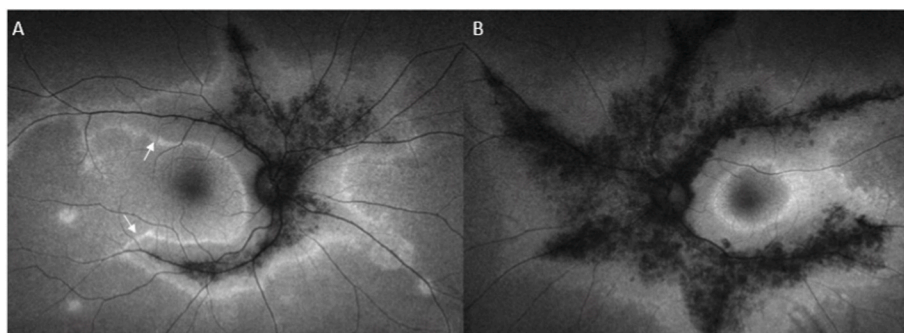


Fig. 2. Fundus autofluorescence (FAF) OD (A) and OS (B) demonstrating a well-demarcated contiguous area of hypoautofluorescence along the venous arcades corresponding to areas of chorioretinal atrophy, with OS being more pronounced than OD. The areas of hypoautofluorescence are surrounded by a ring of hyperautofluorescence.

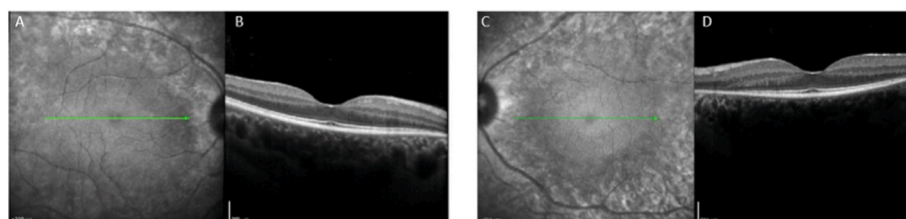


Fig. 3. Infrared *en face* and OCT B-scans of OD (3A&B) and OS (3C&D) demonstrating loss of the outer retina over the affected areas in OU.

choriocapillaris hypoperfusion, which suggests that PPCRA initially affects the choroidal vasculature. On the other hand, Battaglia et al. found that there is reduced vessel density in the deep capillary plexus, and suggest that the initial insult occurs at the retinal circulation in this disease.¹³ In both of these reports, the authors agree that choriocapillaris hypoperfusion is a common endpoint in this disease process.

Our study utilizes clinical *en face* OCT-R to non-invasively image hyalocytes at the vitreoretinal interface using a method that has been previously described in the literature.³¹ The rationale for imaging hyalocytes lies in the fact that they are thought to act as sentinels of activity occurring in the retina below and play significant roles in mediating homeostasis, neuroprotection, and tissue repair.^{24,32} While prior studies of hyalocytes were predominantly performed in animal models using staining or confocal imaging techniques, more recent studies have used clinical OCT and adaptive optics scanning light ophthalmoscopy (AOSLO) to visualize the morphology, physiology, and spatial distribution of these cells at the vitreoretinal interface *in vivo*.^{31,33–36}

Previous studies have suggested that hyalocytes assume various morphologies depending upon their level of activation.³¹ In the advanced “activated” state, hyalocytes become more amoeboid in shape with shorter cell processes clustering in the vicinity of tissue stress or injury.^{31,33} In contrast, in the “quiescent” state, hyalocytes cell bodies appear elongated and their filopodia-like processes become ramified, extending and retracting as they surveil their immediate environment, perhaps expressing anti-inflammatory and neurotrophic factors.³⁷ Castanos et al. demonstrated that hyalocytes localize in the vicinity of large blood vessels and display increased density in eyes with ischemia from either central retinal vein occlusion or proliferative diabetic retinopathy.³¹ Furthermore, they showed that hyalocytes adopt a dendriform morphology in healthy eyes and migrate to areas of metabolic stress in retinopathic eyes. Otero-Marquez et al. demonstrated that hyalocyte morphology shifted to a more quiescent state in a patient with thyroid eye disease as the disease activity decreased with treatment with teprotumumab.³⁷

In our patient, the morphology of the imaged hyalocytes differed between the two eyes. In the left eye, that exhibited more advanced pathology, the hyalocytes appeared more ramified with elongated, spindle-like processes, believed to suggest “quiescence” or absence of

inflammation (Fig. 4F). In contrast, the hyalocytes in the less advanced right eye appeared more activated with an amoeboid morphology, suggesting a greater degree of activation, associated with ongoing inflammation (Fig. 4C). We hypothesize that this difference in appearance may be explained by the stage of chorioretinal degeneration in each eye. In the more advanced eye, the activation of the hyalocytes has peaked and returned to a more resting state, while in the less advanced eye the inflammation is still active.^{31,33}

While the exact pathology for PPCRA is poorly understood, the findings from this case report support the hypothesis that inflammation plays a significant role in its pathophysiology.³³ Hyalocytes anterior to the vitreoretinal interface appear to be a potential biomarker of inflammation in a variety of retinal diseases. It is plausible that the presence of activated hyalocytes in this case indicates an ongoing, active inflammatory process. While the cause of this inflammatory process is unclear it likely relates to the same process responsible for creating the previously documented choriocapillaris hypoperfusion in this disease. Whether the inflammation is responsible for the ischemia or the other way around is still unclear.

4. Conclusions

Our case illustrates the use of clinical OCT to image hyalocyte activity in PPCRA, which may be a potential biomarker of the activity and ongoing progression of the disease. Our findings are consistent with an inflammatory etiology for this disease. As further clinical observations of hyalocytes are made in more disease states the exact role of these cells play may become more evident.

Patient consent

The patient consented to publication of the case orally.

Funding

This report was supported by the National Institutes of Health under award numbers R01HL159116 and R01EY027301. Additional funding for this research was provided by the New York Eye and Ear

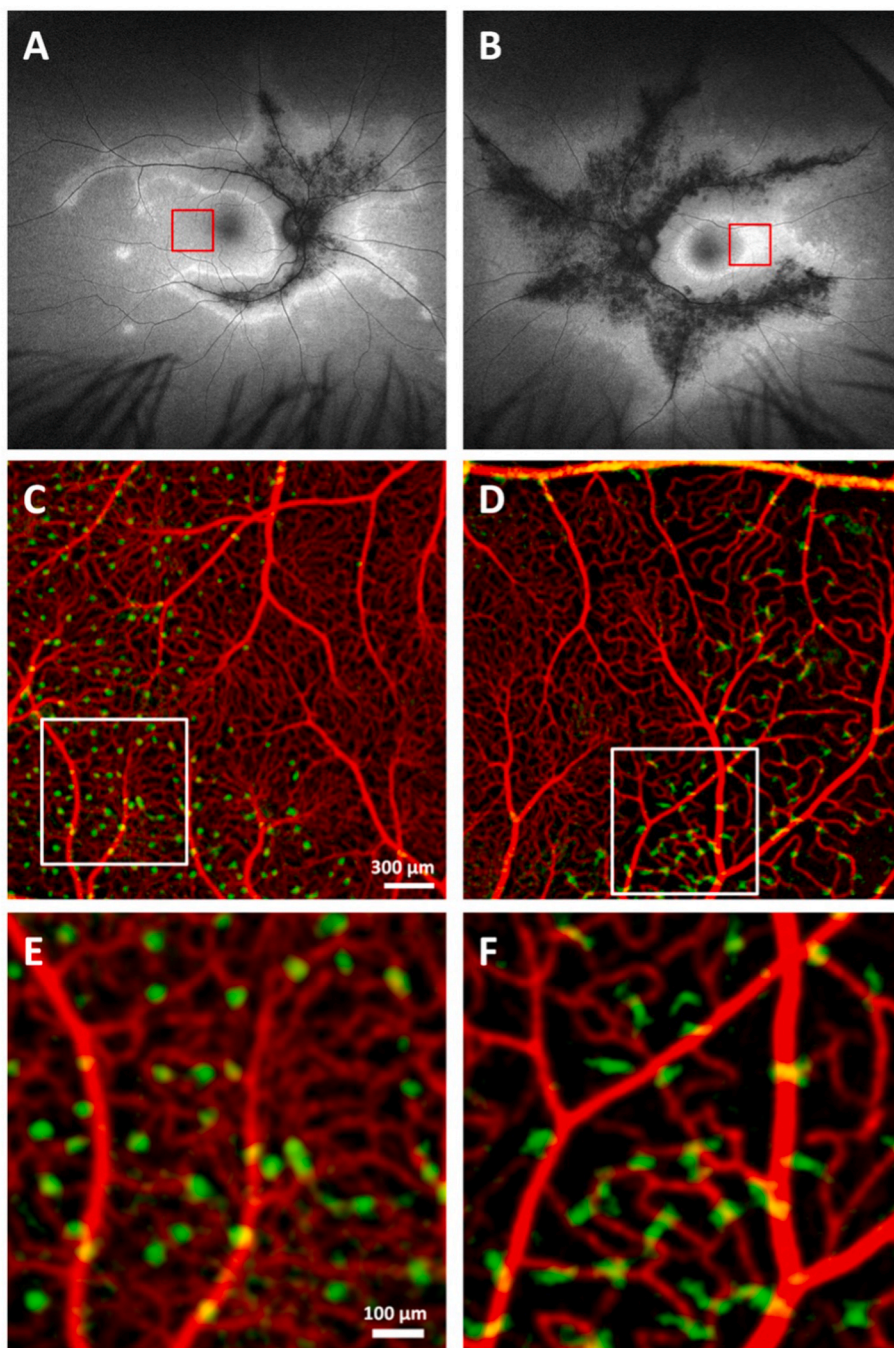


Fig. 4. Fundus autofluorescence (FAF) OD (A) and OS (B). (C, D) Color overlay of 3 mm × 3 mm OCT-A (in red) of retinal vascular layer ILM to OPL + 9 μm and OCT-R (in green) of a 3 μm slab anterior to the ILM at 9° temporal to the fovea OU corresponding to the red squares marked in A and B, respectively. There is decreased capillary density shown in the temporal half of the image OS (D). (E, F) Magnified color overlays of the white box in C and D show hyalocytes located above the ILM in green and retinal capillaries in red, respectively. The morphology of the hyalocytes differ between the fellow eyes, with activated amoeboid-shaped hyalocytes with fewer, retracted processes in the right eye and resting more elongated, ramified hyalocytes in the left eye. (For interpretation of the references to color in this figure legend, the reader is referred to the Web version of this article.)

InfirmityFoundation Grant, the Marrus Family Foundation, the Challenge Grant award from Research to Prevent Blindness, and the Jorge N. Buxton Microsurgical Foundation. The sponsors and funding organizations had no role in the design or conduct of this research. The content is solely the responsibility of the authors and does not necessarily represent the official views of the National Institutes of Health.

Authorship

All authors attest that they meet the current ICMJE criteria for Authorship.

Declaration of competing interest

Richard B. Rosen MD has the following commercial relationships to

declare: Optovue: Code C (Consultant); Astellas: Code C; (Consultant); Boehringer-Ingelheim: Code C (Consultant); CellView: Code C; OD-OS: Code C; Opticology: Code I (Personal Financial Interest); Regeneron: Code C; Lumithera: Code C (Consultant); Guardian Health: Code C (Consultant); Bayer: Code C (Consultant); Genentech-Roche: Code C (Consultant).

The following authors have no financial disclosures: JF, SA, OO, HR, MP, TC.

Appendix A. Supplementary data

Supplementary data to this article can be found online at <https://doi.org/10.1016/j.ajoc.2023.101846>.

References

1. Tsang SH, Sharma T. Pigmented paravenous chorioretinal atrophy (PPCRA). In: *Atlas of Inherited Retinal Diseases*. 2018:111–112.
2. Choi WJ, Joo Kwangsic, KHP. Pigmented paravenous retinochoroidal atrophy. *Kor J Ophthalmol*. 2020;34(1):90–91.
3. Choi JY, Sandberg MA, Berson EL. Natural course of ocular function in pigmented paravenous retinochoroidal atrophy. *Am J Ophthalmol*. 2006;141(4):763–765.
4. Huang H Bin, Zhang YX. Pigmented paravenous retinochoroidal atrophy (review) *Exp Ther Med*. 2014;7(6):1439–1445.
5. Noble KG, Carr RE. Pigmented paravenous chorioretinal atrophy. *Am J Ophthalmol*. 1983;96(3):338–344.
6. Brown T. Retinochoroiditis radiata. *Br J Ophthalmol*. 1937;12:645–648.
7. Chi HH. Retinochoroiditis radiata. *Am J Ophthalmol*. 1948;31(11):1485–1487.
8. Traboulsi EL, Maumenee IH. Hereditary pigmented paravenous chorioretinal atrophy. *Ophthalmic Genet*. 1986;104:1636, 1940.
9. Yamaguchi K, Hara S, Tanifuji Y, Tamai M. Inflammatory pigmented paravenous retinochoroidal atrophy. *Br J Ophthalmol*. 1989;73:463–467.
10. Shona OA, Islam F, Robson AG, Webster AR, Moore AT, Michaelides M. Pigmented paravenous chorioretinal atrophy—detailed clinical study of a large cohort. *Retina*. 2019;39(3):514–529.
11. Batioğlu F, Atmaca LS, Atilla H, Arslanpençe A. Inflammatory pigmented paravenous retinochoroidal atrophy. *Eye*. 2002;16(1):81–84.
12. Lee EK, Lee SY, Oh BL, Yoon CK, Park UC, Yu HG. Pigmented paravenous chorioretinal atrophy: clinical spectrum and multimodal imaging characteristics. *Am J Ophthalmol*. 2021;224:120–132.
13. Battaglia Parodi M, Arrigo A, Chowers I, et al. Optical coherence tomography angiography findings in pigmented paravenous chorioretinal atrophy. *Retina*. 2022;42(5):915–922.
14. Cicinelli MV, Giuffrè C, Rabiolo A, Parodi MB, Bandello F. Optical coherence tomography angiography of pigmented paravenous retinochoroidal atrophy. *Ophthalmic Surg Lasers Imag Retin*. 2018;49(5):381–383.
15. Jung I, Lee Y, Kang S, Won J. Pigmented paravenous retinochoroidal atrophy: a case report supported by multimodal imaging studies. *Med*. 2021;57(12).
16. Shen Y, Xu X, Cao H. Pigmented paravenous retinochoroidal atrophy: a case report. *BMC Ophthalmol*. 2018;18(1):1–4.
17. Sebag J. Vitreous and vitreoretinal interface. In: *Ryan's RETINA*. sixth ed. 2018: 544–581. Cleveland.
18. Kita T, Hata Y, Ishibashi T. Hyalocytes. In: *Encyclopedia of the Eye*. 2010:251–256.
19. Bringmann A, Pannicke T, Grosche J, et al. Müller cells in the healthy and diseased retina. *Prog Retin Eye Res*. 2006;25(4):397–424.
20. Vagaja NN, Chinnery HR, Binz N, Kezic JM, Rakoczy EP, McMenamin PG. Changes in murine hyalocytes are valuable early indicators of ocular disease. *Investig Ophthalmol Vis Sci*. 2012;53(3):1445–1451.
21. Santos AM, Calvente R, Tassi M, et al. Embryonic and postnatal development of microglial cells in the mouse retina. *J Comp Neurol*. 2008;506:224–239.
22. Ogawa K. Scanning electron microscopic study of hyalocytes in the Guinea pig eye. *Arch Histol Cytol*. 2002;65(3):263–268.
23. Lazarus HS. *Hyalocytes*. 2022.
24. Chen L, Yang P, Kijlstra A. Distribution, markers, and functions of retinal microglia. *Ocul Immunol Inflamm*. 2002;10(1):27–39.
25. Boneva SK, Wolf J, Rosmus DD, et al. Transcriptional profiling uncovers human hyalocytes as a unique innate immune cell population. *Front Immunol*. 2020:1–14, 11(September).
26. Wolf J, Boneva S, Rosmus DD, et al. Deciphering the molecular signature of human hyalocytes in relation to other innate immune cell populations. *Investig Ophthalmol Vis Sci*. 2022;63(3).
27. Jia Y, Tan O, Tokayer J, et al. Split-spectrum amplitude-decorrelation angiography with optical coherence tomography. *Opt Express*. 2012;20(4):4710.
28. Mo S, Phillips E, Krawitz BD, et al. Visualization of radial peripapillary capillaries using optical coherence tomography angiography: the effect of image averaging. *PLoS One*. 2017;12(1):1–17.
29. Ranjan R, Jain MA, Verghese S, Manayath GJ, Narendran V. Multimodal imaging of pigmented paravenous retinochoroidal atrophy. *Eur J Ophthalmol*. 2022;32(1): NP125–N129.
30. Gasparian S, Sierpina DI. Fundus autofluorescence detects subtle pigmentary alterations in pigmented paravenous retinochoroidal atrophy. *Am J Ophthalmol Case Reports*. 2021;23, 101158.
31. Castanos MV, Zhou DB, Linderman RE, et al. Imaging of macrophage-like cells in living human retina using clinical OCT. *Investig Ophthalmol Vis Sci*. 2020;61(6).
32. Lazarus HS, Hageman GS. In situ characterization of the human hyalocyte. *Arch Ophthalmol*. 1994;112:1356–1962.
33. Migacz JV, Otero-Marquez O, Zhou R, et al. Imaging of vitreous cortex hyalocyte dynamics using non-confocal quadrant-detection adaptive optics scanning light ophthalmoscopy in human subjects. *Biomed Opt Express*. 2022;13(3):1755.
34. Ong JX, Nesper PL, Fawzi AA, Wang JM, Lavine JA. Macrophage-like cell density is increased in proliferative diabetic retinopathy characterized by optical coherence tomography angiography. *Investig Ophthalmol Vis Sci*. 2021;32(10).
35. Wieghofer P, Engelbert M, Chui TYP, Rosen RB, Sakamoto T, Segaf J. Hyalocyte origin, structure, and imaging. *Expet Rev Ophthalmol*. 2022:1–16.
36. Jones CH, Gui W, Schumann RG, Boneva SK, Lange CAK. Hyalocytes in proliferative vitreo-retinal diseases. *Expet Rev Ophthalmol*. 2022:1–18.
37. Otero-Marquez O, Fayad M, Pinhas A, Chui TYP, Rosen RB, Reddy HS. Retinal surface macrophage changes in thyroid eye disease before and after treatment with teprotumumab. *Case Rep Ophthalmol Med*. 2022:1–5.